Reactivity of a Terminal Ti(IV) Imido Complex toward Alkenes and Alkynes: Cycloaddition vs C−H Activation

Jennifer L. Polse, Richard A. Andersen,* and Robert G. Bergman*

Contribution from the Department of Chemistry, University of California, Berkeley, California 94720

Received April 30, 1998

Abstract: This paper describes the reactivity of the base-free titanium imido complex $Cp^*_2Ti{=}NPh$ (**1**) (Cp^* = pentamethylcyclopentadienyl) toward alkenes and alkynes. Complex **1** reacts with ethylene and acetylene to generate the azametallacycles $Cp^*_2Ti(N(Ph)CH_2CH_2)$ (**2**) and $Cp^*_2Ti(N(Ph)CH{=}CH)$ (**3**), respectively. In the case of ethylene, the cycloaddition is readily reversible, and **2** was characterized spectroscopically under an ethylene atmosphere. We have also examined the reactivity of **1** toward phenyl- and trimethylsilylacetylene and have found that **1** activates the alkynyl C−H bond to give anilido−acetylide complexes $Cp^*_2Ti(N(Ph)H)C{\equiv}CR$ (**6**, R = Ph; **7**, R = $SiMe_3$). This reaction proceeds without observable intermediate metallacyclobutene complexes such as those observed previously for the reaction of the related oxo complex $Cp^*_2Ti(O)pyr$ (pyr = pyridine) with terminal alkynes. Thermolysis of azametallacyclobutene **3** results in formation of the novel ring-activated complex $Cp^*(\eta^5,\eta^1\text{-}C_5Me_4CH_2CH{=}CH)TiN(Ph)H$ (**5**).

Introduction

Complexes containing metal−nitrogen multiple bonds are ubiquitous in transition-metal chemistry.[1−4] These compounds, which are most often found for metals in the middle of the transition series, such as Mo, W, and Re, rarely display reactivity at the M=N bond. Notable exceptions are the growing number of imido complexes of both later[5−10] and earlier[11−31] transition metals, especially group IV imido complexes. Their reactions include C−H activation,[16,20,26,28] cycloadditions of unsaturated C−C and C−X bonds,[24−26,28−30] and addition of H_2 and alkylsilanes.[32,33] Group IV imido complexes participate in imine metathesis[24,25] and catalyze the hydroamination of alkynes to enamines.[30,34] The isoelectronic group IV oxo complexes are products of numerous other Zr- and Ti-mediated organic transformations, including ketone olefinations[35,36] and the chain-termination step of ring-opening metathesis polymerization (ROMP).[37] These complexes are usually generated by cycloreversion of oxa- or azametallacycles which are not isolable.[35,38] In most cases the oxo or imido complexes rapidly decompose

(1) Nugent, W. A.; Haymore, B. L. *Coord. Chem. Rev.* **1980**, *31*, 123.
(2) Nugent, W. A.; Mayer, J. M. *Metal−Ligand Multiple Bonds*; Wiley: New York, 1988.
(3) Mountford, P. *Chem. Commun.* **1997**, 2127.
(4) Wigley, D. E. *Prog. Inorg. Chem.* **1994**, *42*, 239.
(5) Michelman, R. I.; Andersen, R. A.; Bergman, R. G. *J. Am. Chem. Soc.* **1991**, *113*, 5100.
(6) Michelman, R. I.; Ball, G. E.; Bergman, R. G.; Andersen, R. A. *Organometallics* **1994**, *13*, 869.
(7) Glueck, D. S.; Wu, J.; Hollander, F. J.; Bergman, R. G. *J. Am. Chem. Soc.* **1991**, *113*, 2041.
(8) Burrell, A. K.; Steedman, A. J. *J. Chem. Soc., Chem. Commun.* **1995**, 2109.
(9) Kee, T. P.; Park, L. Y.; Robbins, J.; Schrock, R. R. *J. Chem. Soc., Chem. Commun.* **1991**, 121.
(10) Danapoulos, A. A.; Wilkinson, G.; Hussainbates, B.; Hursthouse, M. B. *Polyhedron* **1992**, *11*, 2961.
(11) Roesky, H. W.; Voelker, H.; Witt, M.; Noltemeyer, M. *Angew. Chem., Int. Ed. Engl.* **1990**, *29*, 669.
(12) Berreau, L. M.; Young, V. G.; Woo, L. K. *Inorg. Chem.* **1995**, *34*, 527.
(13) Duchatearu, R.; Williams, A. J.; Gambarotta, S.; Chiang, M. Y. *Inorg. Chem.* **1991**, *30*, 4863.
(14) Lewkebandara, T. S.; Sheridan, P. H.; Heeg, M. J.; Rheingold, A. L.; Winter, C. H. *Inorg. Chem.* **1994**, *33*, 5879.
(15) Winter, C. H.; Sheridan, P. H.; Lewkebandara, T. S.; Heeg, M. J.; Proscia, J. W. *J. Am. Chem. Soc.* **1992**, *114*, 1095.
(16) Cummins, C. C.; Schaller, C. P.; Duyne, G. D. V.; Wolczanski, P. T.; Chan, A. W. E.; Hoffmann, R. *J. Am. Chem. Soc.* **1991**, *113*, 2985.
(17) Hill, J. E.; Profilet, R. D.; Fanwick, P. E.; Rothwell, I. P. *Angew. Chem., Int. Ed. Engl.* **1990**, *29*, 664.
(18) Hill, J. E.; Fanwick, P. E.; Rothwell, I. P. *Inorg. Chem.* **1991**, *30*, 1143.
(19) Doxsee, K. M.; Garner, L. C.; Juliette, J. J. J.; Mouser, J. K. M.; Weakley, T. J. R.; Hope, H. *Tetrahedron* **1995**, *51*, 4321.
(20) Cummins, C. C.; Baxter, S. M.; Wolczanski, P. T. *J. Am. Chem. Soc.* **1988**, *110*, 8731.
(21) Dunn, S. C.; Batzanov, A. S.; Mountford, P. *J. Chem. Soc. Chem. Commun.* **1994**, 2007.
(22) Profilet, R. D.; Zambrano, C. H.; Fanwick, P. E.; Nash, J. J.; Rothwell, I. P. *Inorg. Chem.* **1990**, *29*, 4362.
(23) Arney, D. J.; Bruek, M. A.; Huber, S. R.; Wigley, D. E. *Inorg. Chem.* **1992**, *31*, 3749.
(24) Meyer, K. E.; Walsh, P. J.; Bergman, R. G. *J. Am. Chem. Soc.* **1995**, *117*, 974.
(25) Meyer, K. E.; Walsh, P. J.; Bergman, R. G. *J. Am. Chem. Soc.* **1994**, *116*, 2669.
(26) Walsh, P. J.; Hollander, F. J.; Bergman, R. G. *Organometallics* **1993**, *12*, 3705.
(27) Doxsee, K. M.; Farahi, J. B.; Hope, H. *J. Am. Chem. Soc.* **1991**, *113*, 8889.
(28) Walsh, P. J.; Hollander, F. J.; Bergman, R. G. *J. Am. Chem. Soc.* **1988**, *110*, 8729.
(29) Bennett, J. L.; Wolczanski, P. T. *J. Am. Chem. Soc.* **1994**, *116*, 2179.
(30) Walsh, P. J.; Baranger, A. M.; Bergman, R. G. *J. Am. Chem. Soc.* **1992**, *114*, 1708.
(31) Dunn, S. C.; Mountford, P.; Shishkin, O. V. *Inorg. Chem.* **1996**, *35*, 1006.
(32) Smith, M. R., III; Ball, G. E.; Andersen, R. A. To be submitted for publication.
(33) Lee, S. Y.; Bergman, R. G. Unpublished results.
(34) Taube, R. In *Homogeneous Catalysis with Organometallic Compounds*; Cornils, B., Herrmann, W. A., Eds.; VCH: Weinheim, 1996.
(35) Brown-Wensley, K. A.; Buchwald, S. L.; Cannizzo, L.; Clawson, L.; Ho, S.; Meinhardt, D.; Stille, J. R.; Straus, D.; Grubbs, R. H. *Pure Appl. Chem.* **1983**, *55*, 1733.
(36) Hughes, D. L.; Payack, J. F.; Cai, D.; Verhoeven, T. R.; Reider, P. J. *Organometallics* **1996**, *15*, 663.
(37) Petasis, N.; Fu, D.-K. *J. Am. Chem. Soc.* **1993**, *115*, 7208.
(38) Jørgensen, K. A.; Shiøtt, B. *Chem. Rev.* **1990**, *90*, 1483.

10.1021/ja981489n CCC: $15.00
Published on Web 12/10/1998

Scheme 1

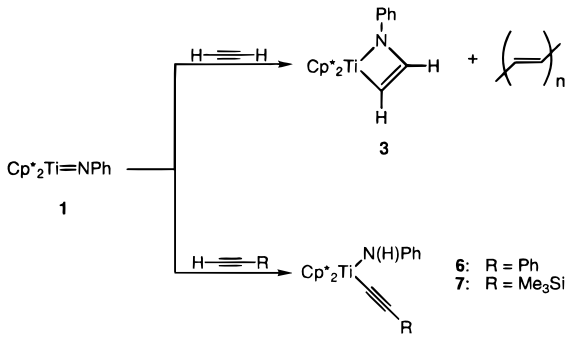

to poorly defined polymeric species, complicating detailed studies of their reactivity.

We recently described the synthesis of the base-free titanocene imido complex $Cp^*_2Ti{=}NPh$ ($Cp^* = Me_5C_5$) (**1**) from the reaction of $Cp^*_2Ti(C_2H_4)$[39] and PhN_3 (eq 1).[32] We report here that **1** reacts with ethylene and acetylene to generate the azametallacycles $Cp^*_2Ti(N(Ph)CH_2CH_2)$ (**2**) (eq 2) and $Cp^*_2Ti(N(Ph)CH{=}CH)$ (**3**) (Scheme 1), respectively. We have also

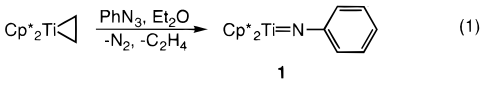

examined the reactivity of **1** with phenyl- and trimethylsilylacetylene and have found that, in contrast to its reaction with acetylene, **1** activates the alkynyl C−H bond of these alkynes to give anilido−acetylide complexes.

Results

Reversible [2 + 2] Cycloaddition of $Cp^*_2Ti{=}NPh$ (1) with Ethylene. Addition of excess ethylene to **1** generates a new complex, **2**, that exists in rapid equilibrium with **1** and free ethylene at room temperature (eq 2). The variable-temperature ^1H NMR spectra of this mixture are shown in Figure 1. In the

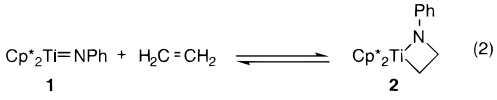

presence of 3 equiv of ethylene, no resonances for **1** are observed below −40 °C, at which temperature the equilibrium strongly favors **2**. Complex **2** gives broad signals in the ^1H NMR spectrum between 25 and −40 °C due to the equilibrium shown in eq 2 (vide infra). This intermolecular exchange process is frozen out on the ^1H NMR time scale at −50 °C in toluene-d_8 to give a spectrum of **2** consisting of a singlet for the Cp* protons at 1.67 ppm, phenyl resonances integrating to one proton each at 7.35, 7.24, 6.79, 6.50, and 6.19 ppm, and two second-order multiplets integrating to two protons each at 2.35 and 1.82 ppm. In addition there is a sharp singlet for free ethylene at 5.30 ppm. The $^{13}C\{^1H\}$ NMR spectrum at −50 °C exhibits two methylene resonances, assigned by standard DEPT pulse sequences, at 64.3 and 25.5 ppm. A one-bond $^1H-^{13}C$ HMQC[40] NMR spectrum showed that the two methylene resonances are coupled to the second-order multiplets in the ^1H NMR spectrum ($^1J_{C-H} = 139$ and 135 Hz, respectively). Complex **2** is stable in solution for several months when stored at −50 °C under an ethylene atmosphere. Removing the ethylene atmosphere under

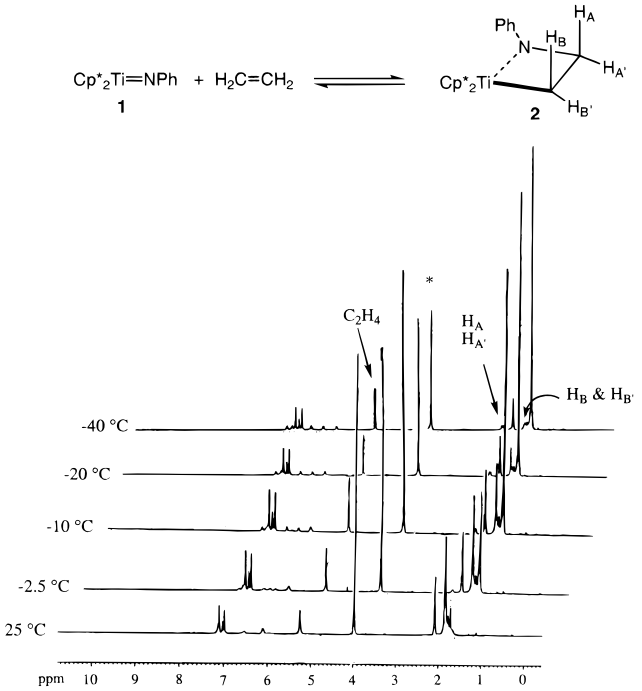

Figure 1. Variable-temperature ^1H NMR spectra of $Cp^*_2Ti{=}NPh$ (**1**) + C_2H_4. The peak marked with an asterisk is Cp_2Fe.

dynamic vacuum or warming the reaction mixture above 25 °C regenerates **1** quantitatively.

Nitrogen-15-labeled **2**, prepared from $Cp^*_2Ti{=}^{15}NPh$,[32] was synthesized in order to obtain the coupling constants between the methylene hydrogens and nitrogen. A long range $^1H-^{15}N$ HMBC[41] spectrum acquired at −80 °C revealed that only the downfield methylene resonance was coupled to ^{15}N ($J_{N-H} \leq 3$ Hz); this coupling was not resolved in the 1D ^1H NMR spectrum. Curiously, no coupling of the ^{15}N to the methylene carbons was observed in the low-temperature $^{13}C\{^1H\}$ NMR spectrum of the ^{15}N-labeled complex. Values for one-bond $^{15}N-^{13}C$ coupling constants are typically ∼10 Hz and can decrease if the atoms are constrained in a ring.[42] We therefore attribute our failure to observe this coupling to the relatively broad lines in the $^{13}C\{^1H\}$ NMR spectrum. Labeling with $^{13}C_2H_4$ allowed us to measure a $^1J_{C-C}$ of 27 Hz for the methylene carbons. The small value for $^1J_{C-C}$ is consistent with the presence of sp^3 carbons constrained in a ring.[43] On the basis of the above data, **2** is formulated as the azametallacyclobutane complex $Cp^*_2Ti(N(Ph)CH_2CH_2)$ (eq 2) rather than as the isomeric π-complex.

In complex **2** both of the inequivalent methylene resonances remain well separated for all temperatures at which the complex is observable. This is in contrast to the low-temperature coalescence of the methylene sites that has been observed in other azametallacyclobutane complexes.[26,29,44] To assess whether exchange between the metallacycle methylenes was occurring slowly on the NMR time scale, a $^1H-^1H$ EXSY[45,46] spectrum of **2** under 1 atm of ethylene was acquired at 0 °C (Figure 2). The presence of cross-peaks between protons A and B (see Figure 1 for labeling scheme) indicates that exchange between

(39) Cohen, S. A.; Auburn, P. A.; Bercaw, J. E. *J. Am. Chem. Soc.* **1983**, *105*, 1136.
(40) Bax, A.; Subramanian, S. *J. Magn. Reson.* **1986**, *67*, 565.
(41) Bax, A.; Summers, M. F. *J. Am. Chem. Soc.* **1986**, *108*, 2093.
(42) Wasylishen, R. E. *Can. J. Chem.* **1976**, *54*, 833.
(43) Abraham, R. J.; Loftus, P. *Proton and Carbon-13 NMR Spectroscopy An Integrated Approach*; Heyden and Son Ltd.: Philadelphia, PA, 1979; p 230.
(44) de With, J.; Horton, A. D.; Orpen, A. G. *Organometallics* **1993**, *12*, 1493.
(45) Jeener, J.; Meier, B. H.; Bachmann, P.; Ernst, R. R. *J. Phys. Chem.* **1979**, *71*, 4546.
(46) Meier, B. H.; Ernst, R. R. *J. Am. Chem. Soc.* **1979**, *101*, 6441.

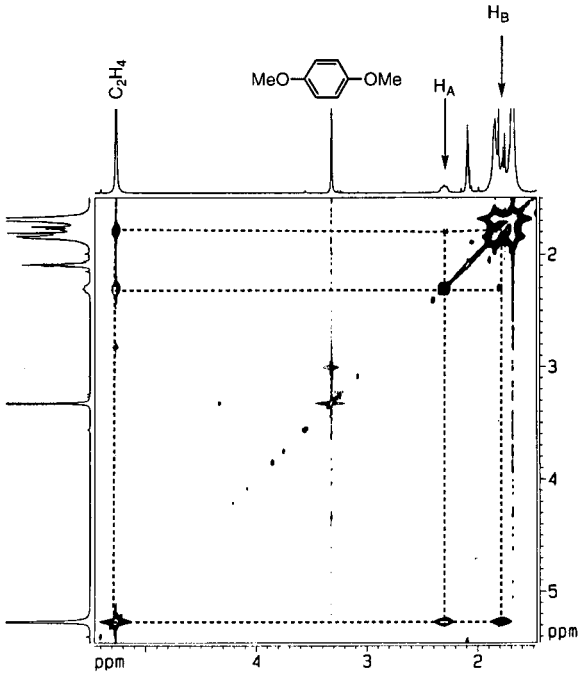

Figure 2. EXSY NMR spectrum of $Cp^*_2Ti(NH(Ph)CH_2CH_2)$ (**2**) equilibrating with $Cp^*_2Ti{=}NPh$ (**1**) and C_2H_4 at 0 °C. Dimethoxybenzene was added as an internal standard. The spectrum was recorded with a mixing time of 80 ms. Other parameters and experimental details are given in the Experimental Section.

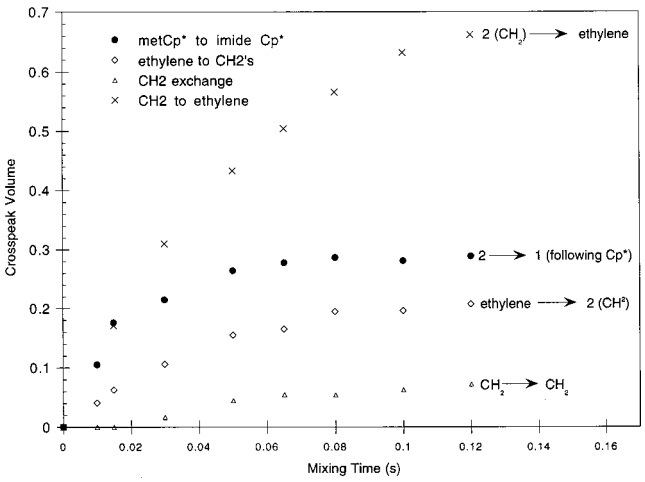

Figure 3. Plots of cross-peak volume vs τ_m obtained from EXSY spectra of the reaction shown in eq 2. Spectra were recorded and analyzed as described in the Experimental Section. Rate constants were estimated from the initial slopes and are shown in Table 1.

the two methylene sites does occur on the EXSY time scale. Cross-peaks are also observed between the free ethylene resonance and both methylene resonances, indicating that cycloreversion to **1** and free ethylene is occurring on the NMR time scale at this temperature.

To gain further insight into the nature of these exchange processes, a series of EXSY spectra with varying mixing times, τ_m, were acquired. A plot of cross-peak volume vs τ_m for the various exchange processes is shown in Figure 3. There is an induction period of 30 ms prior to observation of a cross-peak between the methylene resonances. This is characteristic of relayed magnetization and indicates that the methylene sites do not undergo direct exchange.[47] The most likely explanation is

(47) Ramachandran, R.; Knight, C. T. G.; Kirkpatrick, R. J.; Oldfield, E. *J. Magn. Reson.* **1985**, *65*, 136.

Table 1. Rate Data for the Interconversion of **1** and C_2H_4 with **2**

site A	site B	$k_{A\rightarrow B}$ (s^{-1})	rate × rel concn (M/L/s)
2	1	9.64 ± 2.31	0.163 ± 0.078
2 (methylenes)	C_2H_4	14.8 ± 1.74	0.251 ± 0.030
C_2H_4	**2** (methylenes)	5.56 ± 0.68	0.246 ± 0.024

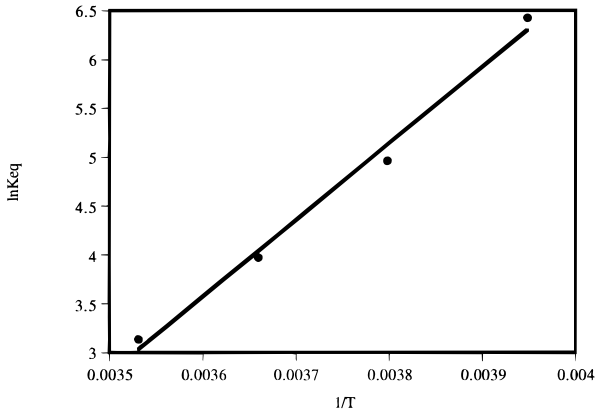

Figure 4. Van't Hoff plot for the equilibration of **2** with **1** and C_2H_4 between 10 and −20 °C. Points were obtained as described in the Experimental Section.

that methylene exchange occurs via free ethylene (vide infra). Repetition of the experiments with 5 equiv of free ethylene results in substantial lengthening of this induction period (200 ms), consistent with increased dilution of the transferred magnetization in the pool of free ethylene. The initial pseudo-first-order rate constants for the exchange process (Table 1) were obtained from the initial slopes of the lines shown in Figure 3.[47] A van't Hoff plot (Figure 4) constructed from NMR data taken between 10 and −20 °C gives $\Delta H° = -15.6 \pm 1.1$ kcal/mol, $\Delta S° = -48.9 \pm 10.0$ eu, and $\Delta G° = -2.2 \pm 2.9$ kcal/mol for the reaction of **1** with ethylene at 0 °C.

[2 + 2] Cycloaddition of 1 with Acetylene. Passing acetylene gas through a room-temperature benzene solution of **1** results in an instantaneous color change due to formation of the deep violet air- and moisture-sensitive azametallacyclobutene complex $Cp^*_2Ti(N(Ph)CH{=}CH)$ (**3**) (Scheme 1) which was isolated in 62% yield. Reaction times longer than 5 min lead to precipitation of a deep red powder, insoluble in all standard solvents, that is presumed to be polyacetylene. Treatment of isolated **3** with acetylene gas also results in formation of the red powder with no noticeable decomposition of **3**.

The room-temperature ^1H NMR spectrum of **3** in toluene-d_8 exhibits broad peaks for the *o*- and *m*-phenyl resonances. Cooling to −10 °C freezes the Ph−N rotation on the NMR time scale, and all five chemically inequivalent resonances are resolved. In the ^1H NMR spectrum the metallacycle ring methine resonances appear as two doublets ($^3J_{HH} = 9$ Hz) at 7.02 and 7.08 ppm. The $^{13}C\{^1H\}$ NMR spectrum shows a characteristic low-field resonance at 186.2 ppm for the vinylic carbon bonded to titanium;[48] the second methine carbon appears at 96.8 ppm.

The identity of **3** as a metallacyclobutene complex rather than an acetylene adduct in the solid state was confirmed by a single-crystal X-ray diffraction study. Details of the study are given in the Experimental Section and as Supporting Information. An ORTEP diagram of **3** is shown in Figure 5. Selected bond lengths and angles are provided in Tables 2 and 3. The metallacycle ring is planar and the phenyl group on the nitrogen

(48) Doxsee, K. M.; Juliette, J. J. J.; Weakley, T. J. R.; Zientara, K. *Inorg. Chim. Acta* **1994**, *222*, 305 and references therein.

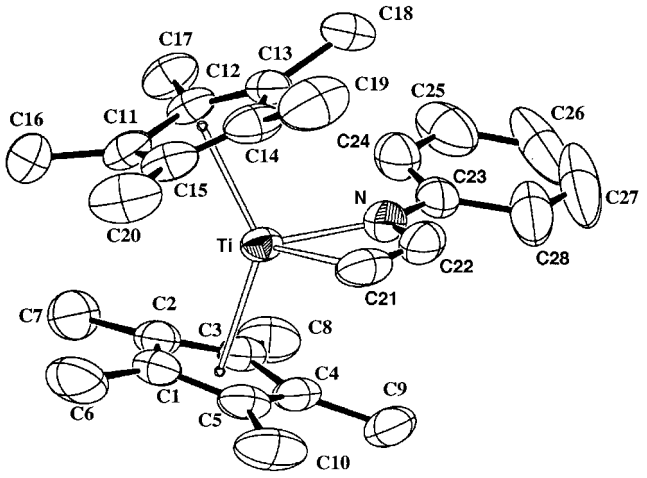

Figure 5. ORTEP diagram of $Cp^*_2Ti(NH(Ph)CH{=}CH)$ (**3**).

Table 2. Selected Intramolecular Distances for **3** and **6**

	distance (Å)
Complex **3**	
Ti−N	2.059(2)
Ti−C21	2.060(2)
Ti−Cp^{*1}	2.1172(3)
Ti−Cp^{*2}	2.1159(3)
C21−C22	1.326(3)
N−C22	1.417(3)
N−C23	1.393(3)
Complex **6**	
Ti−N	1.993(4)
Ti−C27	2.105(6)
Ti−Cp^{*1}	2.125
Ti−Cp^{*2}	2.126
C27−C28	1.210(6)
C28−C29	1.432(7)
N−C21	1.403(6)
N−H(N)	0.83(4)

Table 3. Selected Intramolecular Angles for **3** and **6**

	angle (deg)
Complex **3**	
Cp^{*1}−Ti−Cp^{*2}	138.18(2)
N−Ti−Cp^{*1}	106.79(5)
N−Ti−Cp^{*2}	110.63(5)
C21−Ti−Cp^{*1}	105.39(6)
C21−Ti−Cp^{*2}	105.04(6)
N−Ti−C21	68.68(9)
Ti−N−C22	86.6(1)
Ti−N−C23	150.3(1)
C22−N−C23	123.1(2)
N−C22−C21	115.8(2)
Complex **6**	
Cp^{*1}−Ti−N	103.00
Cp^{*2}−Ti−N	109.48
Cp^{*1}−Ti−C27	103.06
Cp^{*2}−Ti−C27	101.04
Cp^{*1}−Ti−Cp^{*2}	137.34
N−Ti−C27	94.76(18)
Ti−N−C21	140.5(3)
Ti−N−H(N)	111.9(33)
C21−N−H(N)	107.6(32)
Ti−C27−C28	176.4(4)
C27−C28−C29	179.6(5)

is tilted slightly out of the metallacycle plane, perhaps due to crystal packing forces. We assume the essential planarity at the N atom is due at least partially to delocalization of the lone pair into the aromatic ring.[49] The Ti−C distance of 2.060(2) Å is within the typical range for Ti−C_{sp^2} bonds and is similar to the Ti−C distances of structurally characterized titanacyclobutenes.[50−53] The Ti−N (2.059(2) Å) distance is within the expected range for Ti−N bonds not involving significant π-bonding.[54,55] The C21−C22 distance (1.326(3) Å) clearly indicates a double bond and is similar to the C=C distance in a related zirconium azametallacyclobutene complex Cp_2Zr-(N(Ph)C(Ph)=CPh) (1.361(8) Å).[30]

In contrast to what is observed for **2**, the methine resonances of **3** do not exchange on the NMR time scale between −20 and 70 °C. This is curious since related (albeit substituted) zirconium azametallacyclobutenes[26,28,30] and titanium and zirconium oxametallacyclobutenes[52,56−58] undergo rapid cycloreversion reactions. To determine whether exchange occurs on a longer time scale, a solution of **3** in THF-d_8 was treated with 3 equiv of DC≡CD. After 3 d at room temperature the added acetylene had been converted to polyacetylene with no observable deuterium incorporation into **3**. The lack of deuterium incorporation into the metallacycle indicates that **3** is probably not the active acetylene polymerization catalyst. Because polymerization of added acetylene occurs readily at room temperature and quite rapidly at higher temperatures, experiments designed to probe an equilibrium between **1** and **3** are not feasible.

We reported previously that titanium oxametallacyclobutene complexes rearrange to give hydroxo−acetylide complexes (eq 3).[52,59] To determine whether **3** undergoes a similar rearrangement, a benzene solution of **3** was heated to 45 °C for 14 days.

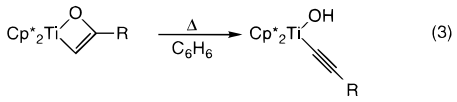

(3)

This thermolysis did not yield the expected anilido-acetylide product, but gave a new complex **5** (Scheme 2), which was isolated in 57% yield after crystallization from hexanes. The ^1H NMR spectrum of **5** shows two second-order multiplets at 2.9 and 3.0 ppm, as well as seven multiplets integrating to one proton each from 6.44 to 7.45 ppm. The inequivalent methyl protons on the C−H-activated Cp* ring were clearly resolved in both the ^1H and $^{13}C\{^1H\}$ NMR spectra. In addition to the expected phenyl and Cp* resonances, the $^{13}C\{^1H\}$ NMR spectrum exhibits a methylene resonance at 33.2 ppm, as well as two methines at 195.9 and 157.2 ppm. The methine resonance at 195.9 ppm is indicative of a vinylic carbon bonded to titanium.[48] An $^1H-^{13}C$ HMQC[40] spectrum showed that the methylene resonance in the $^{13}C\{^1H\}$ NMR spectrum correlates

(49) Osborne, J. H.; Rheingold, A. L.; Trogler, W. C. *J. Am. Chem. Soc.* **1985**, *107*, 7945.
(50) Schwartz, D.; Smith, M. R., III; Andersen, R. A. *Organometallics* **1996**, *15*, 1446.
(51) For examples of structurally characterized titancyclobutenes, see: (a) Tebbe, F. N.; Harlow, R. L. *J. Am. Chem. Soc.* **1980**, *102*, 6151. (b) Beckhaus, R.; Sang, J.; Wagner, T.; Ganter, B. *Organometallics* **1996**, *15*, 1176.
(52) Polse, J. L.; Andersen, R. A.; Bergman, R. G. *J. Am. Chem. Soc.* **1995**, *117*, 5393.
(53) Beckhaus, R.; Strauss, I.; Wagner, T.; Kiprof, P. *Angew. Chem., Int. Ed. Engl.* **1993**, *32*, 264.
(54) Feldman, J.; Calabrese, J. C. *J. Chem. Soc., Chem. Commun.* **1991**, 1042.
(55) Bynum, R. V.; Hunter, W. E.; Rogers, R. D.; Atwood, J. L. *Inorg. Chem.* **1980**, *19*, 2368.
(56) Carney, M. J.; Walsh, P. J.; Hollander, F. J.; Bergman, R. G. *J. Am. Chem. Soc.* **1989**, *111*, 8751.
(57) Carney, M. J.; Walsh, P. J.; Hollander, F. J.; Bergman, R. G. *Organometallics* **1992**, *11*, 761.
(58) Carney, M. J.; Walsh, P. J.; Bergman, R. G. *J. Am. Chem. Soc.* **1990**, *112*, 6426.
(59) For a related azametallacycle-to-alkynylamido complex rearrangement, see: Blake, R. E.; Antonelli, D. M.; Henling, L. M.; Schaefer, W. P.; Hardcastle, K. I.; Bercaw, J. E. *Organometallics* **1998**, *17*, 718.

Scheme 2

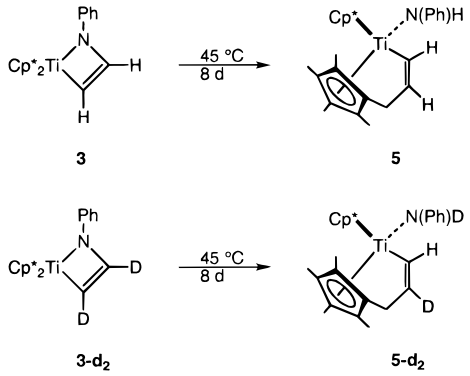

with the two second-order multiplets at 3.0 and 2.9 ppm. A ^{1}H−^{1}H COSY spectrum revealed that the methylene protons were coupled to two multiplets at 7.45 and 7.12 ppm. The HMQC spectrum showed that these low-field multiplets correlate with the methines at 195.9 and 157.2 ppm. The IR spectrum of **5** showed an N−H stretch at 3371 cm^{-1}. On the basis of the above data, **5** was assigned the unusual structure shown in Scheme 2. A single-crystal X-ray diffraction study of **5** confirmed the connectivity of the atoms in the complex, but the anilido fragment is badly disordered and the bond lengths are not reliable.[60]

To probe the mechanism of the rearrangement of **3** to **5**, Cp*$_2$Ti(N(Ph)CD=CD) (**3-d$_2$**) was synthesized by treatment of **1** with acetylene-d_2. Thermolysis of **3-d$_2$** leads to deuterium incorporation at the anilido and β-vinylic positions (Scheme 2). However, examination by ^{2}H and ^{1}H NMR reveals ∼10% scrambling into the Cp* and α-vinylic positions. In addition, the anilido position is ∼10% protiated. Qualitatively, there is no isotope effect on the rearrangement. No crossover was observed when **3-d$_2$** was thermolyzed in the presence of Cp*$_2$Ti(N(tol)CH=CH) (**18**), showing that the reaction is intramolecular.

Reaction of 1 with Terminal Alkynes. Formation of Anilido−Acetylide Complexes. In contrast to its behavior toward acetylene, **1** reacts with phenyl and trimethylsilylacetylene to give the dark brown anilido−acetylide complexes **6** and **7** (Scheme 1). Complex **7** shows C≡C and N−H stretches in the IR at 2721 and 3369 cm^{-1}, respectively, and quaternary carbon resonances for the acetylide ligand at 181 and 159 ppm in the ^{13}C{^{1}H} NMR spectrum. Like the analogous hydroxo−acetylide complex Cp*$_2$Ti(OH)C≡CPh,[52] **6** does not exhibit a C≡C stretch in the IR, although the N−H stretch is visible at 3367 cm^{-1}. In addition, no downfield resonance for the acetylide carbon α to titanium was observed in the ^{13}C{^{1}H} NMR spectrum. Hydrolysis of **6** with 5% HCl in diethyl ether gives phenylacetylene and $PhNH_3Cl$ as the only organic products (formed in >95% yield).

The proposed structure of **6** has been confirmed by X-ray crystallography. An ORTEP diagram is shown in Figure 6, relevant bond lengths and angles are provided in Tables 2 and 3, and details of the structure are given in the Experimental Section or as Supporting Information. The Ti−N distance (1.993(4) Å) is typical of titanium amides,[54,61,62] and there is no intra- or intermolecular hydrogen bonding to the NH group

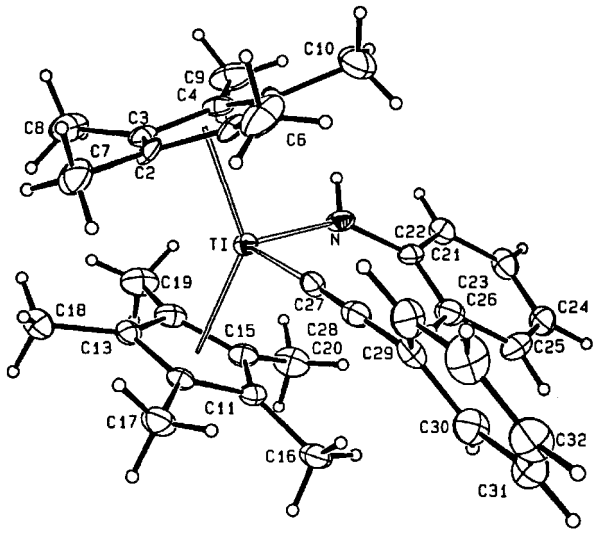

Figure 6. ORTEP diagram of Cp*$_2$Ti(NHPh)C≡CPh. (**6**).

Scheme 3

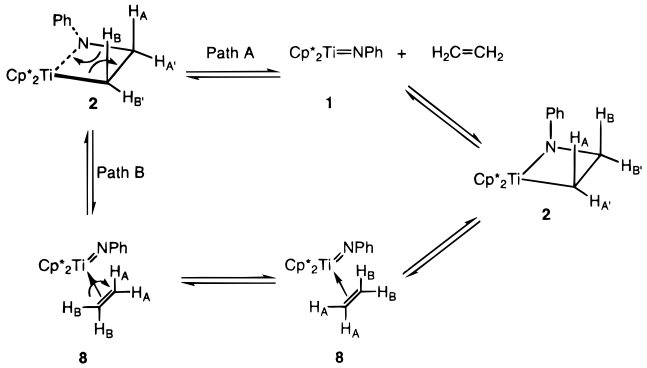

in the solid state. The Ti−C27 distance (2.105(6) Å) compares well to the Ti−C distance of 2.117(2) Å found for Cp*$_2$Ti(OH)C≡CPh.[52] The C27−C28 distance (1.210(6) Å) is clearly a triple bond, as it is similar to the C≡C distance in Cp*$_2$Ti(OH)C≡CPh (1.218(3) Å)[52] and Cp$_2$Zr(C≡CMe)$_2$ (1.206(4) Å).[63]

We previously reported that Cp*$_2$Ti(O)pyr (**4**)[52] reacts with terminal alkynes to give oxametallacyclobutene complexes which then rearrange at higher temperatures to hydroxo−acetylide complexes (eq 3).[52] To look for intermediate azametallacyclobutene complexes in the formation of **6**, 3 equiv of phenylacetylene was added to a precooled solution of **1** in toluene-d_8, and the reaction was followed by ^{1}H NMR at −70 °C. The reaction proceeded rapidly to **6**, with no observable intermediates.

Discussion

Reversible [2 + 2] Cycloaddition of Cp*$_2$Ti=NPh (1) with Ethylene. Treatment of benzene and toluene solutions of **1** with ethylene results in formation of the fluxional azametallacyclobutane complex **2** (eq 2, Scheme 3). This compound, which results from a [2 + 2] cycloaddition of ethylene to the Ti=N bond, is unstable with respect to ethylene loss and could only be characterized in solution at low temperature in the presence of excess ethylene. The ^{1}H, ^{13}C{^{1}H}, and ^{15}N NMR data are consistent with formulation of **2** as a metallacyclobutane complex rather than an ethylene adduct. The chemical shifts

(60) The crystal structure of **5** and tables of positional and thermal parameters and lists of F_o and F_c values for the structures of **3** and **6** are given as Supporting Information.

(61) Lukens, W. W.; Smith, M. R., III; Andersen, R. A. *J. Am. Chem. Soc.* **1996**, *118*, 1719.

(62) Brady, E.; Lukens, W.; Telford, J.; Mitchell, G. *Acta Crystallogr.* **1994**, *C51*, 558.

(63) Erker, G.; Frömberg, W.; Benn, R.; Mynott, R.; Angermund, K.; Krüger, C. *Organometallics* **1989**, *8*, 911.

Scheme 4

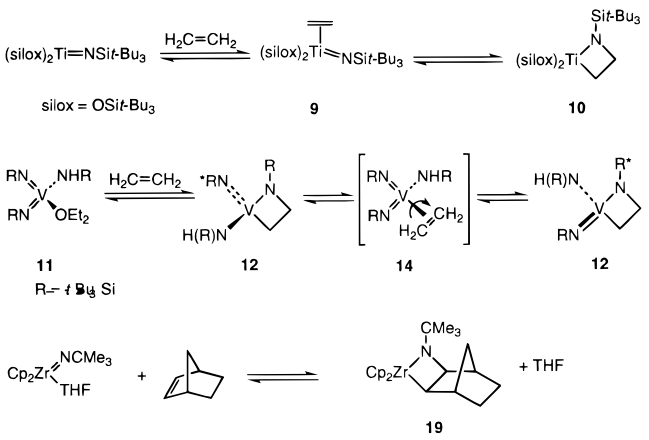

and coupling constants are similar to those of known Ti,[29] Zr,[26] and V azametallacyclobutane complexes.[44] In particular, the methylene resonances occur at chemical shifts that are almost identical to those of the ring methines of structurally characterized Zr azametallacyclobutane complex **19** (Scheme 4),[26] and $^1J_{C-C}$ for the methylenes is greatly reduced relative to its value in free ethylene.[43]

Although the assignment of **2** as the ethylene π-complex **8** (Scheme 3) cannot be definitively ruled out by our data, such a d^0 complex would be expected to be significantly less stable than the cyclized product. In general, d^0 ethylene adducts are destablized due to the lack of back-bonding from the metal center. For example, Wolczanski has estimated that the ethylene adduct, (silox)$_2$Ti(NSitBu_2)(C_2H_4) (**9**), is 8.9 kcal/mol less stable than the azametallacyclobutane complex **10** (Scheme 4).[29] In related work Horton and de With have examined the reaction of vanadium imido complex **11** with ethylene to form the isolable metallacyclobutane complex **12** (Scheme 4).[44] Like **2**, **12** is unstable with respect to ethylene loss, but it was isolated under ethylene at low temperatures.

Our results therefore correspond to the earlier studies summarized above, in that azametallacyclobutanes can be formed and detected, but in general both formation of these complexes and their cycloreversion to imido complexes and alkene are relatively rapid processes. No doubt the low barrier in the Ti and Zr systems is aided by the presence of an empty orbital of a symmetry at the metal center capable of coordinating the alkene (as it does other dative ligands and H_2) and the absence of a large reorganization energy in converting the coordinated alkene to the metallacycle. Exchange appears to be slower only in those systems (e.g., norbornene adduct **19** or metallacyclobutenes formed from alkynes) where the "off" rate is decreased due to thermodynamic stabilization of the rings.

As mentioned above, **2** is fluxional on the NMR time scale. Examination of the 2D EXSY spectrum (Figure 2) of **2** at 0 °C in the presence of ~0.4 equiv of free ethylene reveals that the principal exchange process involves rapid cycloreversion to **1** and free ethylene. Hence, the most intense cross-peaks are observed between the Cp* protons of **1** and **2** and between free ethylene and the methylenes of **2**. It is important to note that exchange between **2** and free ethylene is occurring, but this process is slow enough that the ethylene and methylene resonances are sharp and well separated.

EXSY spectra acquired with longer mixing times ($\tau_m \geq 30$ ms) showed cross-peaks between the two methylene resonances of **2**. Plots of cross-peak volume vs τ_m (Figure 3) revealed that cross-peaks between the methylene resonances appeared only after an induction period of 30 ms. This behavior is characteristic of relayed magnetization and is indicative of a multistep exchange process.[47] EXSY spectra recorded on samples containing much higher concentrations of free ethylene (0.170 M, ~5 equiv) displayed even longer (~200 ms) induction periods prior to observation of methylene exchange cross-peaks. This is consistent with increased dilution of the magnetization of interest within the pool of free ethylene. These experiments indicate that exchange with free ethylene is the lowest energy exchange process, and it is therefore probable that the methylene site exchange occurs via reversible cycloreversion to **1** and free ethylene (Scheme 3, path A). Although a competing pathway involving reversible cycloreversion to freely rotating ethylene adduct **8** (Scheme 3, path B) cannot be ruled out, the data indicate that such a pathway must be significantly slower than complete ethylene dissociation. A similar process which interconverts the hydride and anilido protons of Cp*$_2$Ti(NHPh)(H) **13** (eq 4) will be described in a forthcoming paper.[32] In the imido system, exchange of the amide and hydride positions occurs through reversible, concerted 1,2-elimination of H_2 to form **1** and free H_2 (eq 4).

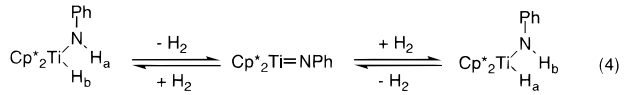

(4)

Despite the similarities to the hydride exchange shown in eq 4, a dissociative exchange mechanism for **2** was somewhat unexpected, since methylene exchange in the related Ti and V azametallacyclobutane complexes has been shown to proceed via a transient ethylene adduct.[29,44] Increasing the ethylene concentration does not affect the rate of methylene exchange in **10** (Scheme 4);[29] this effectively rules out a mechanism involving free ethylene. The methylene resonances in vanadacycle **12** (Scheme 4) were equivalent by ^{1}H NMR even at −90 °C.[44] Since they observed a sharp resonance for free ethylene, the authors concluded that the rapid methylene exchange could not proceed via ethylene loss. They postulated instead that exchange occurred through cycloreversion to transient ethylene complex **14**.

Initial pseudo-first-order rate constants were extracted from the plots of cross-peak volume vs τ_m and are shown in Table 1. Because the cross-peak for methylene exchange arose from relayed magnetization, a rate constant for that process could not be determined by this method. As expected, the product of the rate constant and the relative concentration of the exchanging species are identical within experimental error. A free energy barrier of 14.5 ± 0.8 kcal/mol for the forward process (loss of ethylene from **2**) was calculated from the observed rate constant.

Reactivity of 1 with Alkynes and Rearrangement of 3. As outlined in the Results section, treatment of **1** with acetylene affords **3** in good yield (Scheme 1). Unlike the additions of ethylene and dihydrogen, addition of acetylene across the Ti═N bond of **1** is effectively irreversible. No coalescence of the ring methine resonances was observed by ^{1}H NMR up to 80 °C, and attempts to exchange DC≡CD into **3** resulted in polymerization of the added acetylene without any observable deuterium incorporation. This lack of exchange is very unusual, since group IV aza- and oxametallacyclobutenes typically undergo rapid alkyne exchange reactions.[26,52,56−58] It would appear that **3** is significantly more thermodynamically stable than **1** and acetylene.

Terminal alkynes other than acetylene do not react with **1** to form metallacyclobutenes, but instead form amide acetylide

complexes similar to previously reported hydroxo−acetylide complexes.[52] The preference for C−H activation over cycloaddition is likely steric in origin. The kinetic product of the reaction between terminal alkynes and oxo complex $Cp^*_2Ti(O)$(pyridine) are oxametallacyclobutene complexes. The oxametallacycles rearrange thermally to hydroxo−acetylide complexes (eq 3). This rearrangement was shown to be driven largely by steric effects, since metallacycles derived from larger terminal alkynes rearrange more rapidly.[52] It seems reasonable that **1**, which is already sterically congested due to the imide phenyl group, should strongly prefer the C−H activation pathway over cycloaddition, since formation of an amide acetylide minimizes steric interactions between the imide and alkynyl substituents. We were unable to observe the formation and disappearance of metallacyclobutene complexes during this reaction (even at low temperature), but we cannot rule out such species as transient intermediates. Acetylene is the only terminal alkyne small enough to form a stable cycloaddition product.

Complex **3** is only moderately stable thermally, and prolonged heating at 45 °C results in its rearrangement to the unusual fulvene complex **5** (Scheme 2). Complex **5** can be viewed formally as the product of acetylene insertion into the Ti−C bond of Cp*FvTiNHPh (**15**) (eq 5). Complexes such as **5** which possess Cp or Cp* ligands tethered to a metal center through a pendant side chain have attracted much interest recently as constrained-geometry α-olefin polymerization catalysts.[64−66]

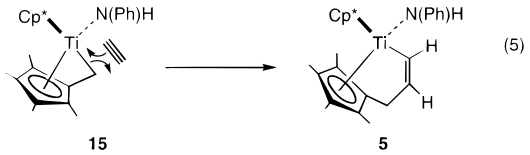

(5)

Such compounds are typically formed from a dianionic ligand and the appropriate metal complex,[64,65] but there have been several reports of new tethered Cp* ligands made by elaboration of a metal−fulvene complex.[67−72] These synthetic routes usually involve insertion of an isonitrile or ketone into the M−C bond of the fulvene to give an amide or alkoxide tether. Luinstra has recently described coupling of fulvene and 2-methylallyl ligands on titanium to give a new tethered Cp* ligand.[68] To our knowledge there have been no reports of alkyne insertion into the M−C bond of a fulvene complex to give an all-carbon unsaturated tether like that of **5**.

Elucidation of the mechanism for the rearrangement of **3** to **6** was hampered by the scrambling of deuterium atoms into the Cp* and α-vinylic positions. It is possible that this scrambling is caused by a trace impurity present in the reaction mixture, although the observed lack of crossover with tolyl derivative **18** makes this unlikely. Two mechanisms that are consistent with the lack of crossover and the observation that deuterium incorporation occurs principally at the anilido and *β*-vinylic

Scheme 5

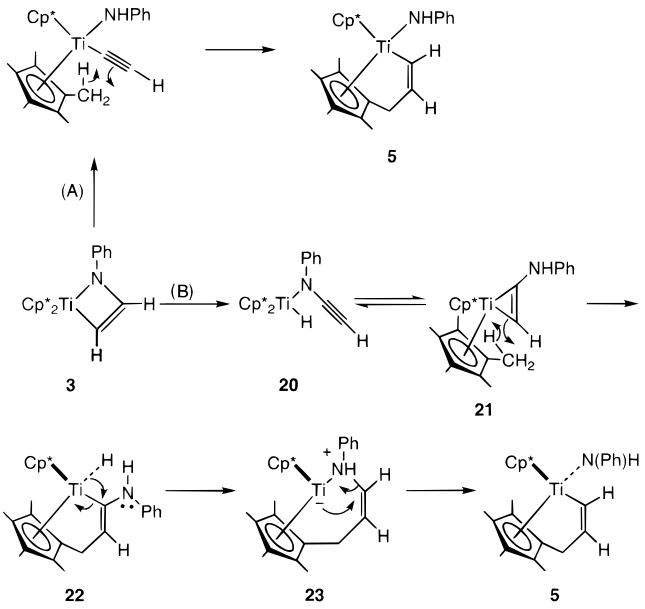

positions are outlined in Scheme 5. Pathway A involves 1,2-migration of H to N with concomitant cleavage of the Ti−C bond, leading to an alkynyl phenylamido complex analogous to **6** and **7**; addition of a Cp* methyl C−H bond across the CC triple bond then gives **5**. Although this is the simpler pathway, the lack of a kinetic isotope effect argues against it, unless the hydrogen migration is preceded by an irreversible (e.g., Ti−C) bond cleavage step. In addition, thermolysis experiments carried out with **6** and **7** demonstrate that these materials are stable to 90 °C, above which they undergo decomposition; no rearrangement to fulvene-type complexes analogous to **5** is observed. In light of the stability of **6** and **7**, it is not clear why the parent anilido complex, if formed, would rearrange so rapidly to **5**. As an alternative, therefore, we offer path B in Scheme 5. This postulates an initial *β*-hydride elimination from **3** (perhaps following initial Ti−C bond cleavage, to facilitate moving the H closer to the metal center, or taking place by two-step migration of H from C to N and then to Ti), leading to intermediate species **20**, which can reductively eliminate to give alkyne complex **21**. Addition of a Cp* methyl group across Ti−C bond of **21** yields hydride intermediate **22**. Coordination of the amine and reductive elimination of the vinyl group yields titanium-ate complex **23**. Attack by titanium followed by cleavage of the N−C bond gives **5**.

Summary

We have shown that imido complex **1** undergoes [2 + 2] cycloaddition reactions with ethylene and acetylene to form the corresponding azametallacyclobutane and azametallacyclobutene complexes **2** and **3**. Compound **2** is unstable with respect to ethylene loss and was characterized in solution by a variety of one- and two-dimensional NMR experiements. The equilibration of **2** with **1** and free ethylene has been studied by variable-temperature NMR. EXSY spectra recorded at several mixing times and two different ethylene concentrations allowed us to measure the rate constant and barrier for ethylene loss. The EXSY spectra also reveal that exchange of the methylene groups in **2** takes place via cycloreversion to **1** and free ethylene.

Although **1** undergoes a cycloaddition reaction with acetylene, it reacts to activate the alkynyl C−H bond of phenyl- and trimethylsilylacetylene to give anilido−acetylide complexes **6**

(64) Devore, D. D.; Timmers, F. J.; Hasha, D. L.; Rosen, R. K.; Marks, T. J.; Deck, P. A.; Stern, C. L. *Organometallics* **1995**, *14*, 3132.
(65) Shapiro, P. J.; Cotter, W. D.; Schaefer, W. P.; Labinger, J. A.; Bercaw, J. E. *J. Am. Chem. Soc.* **1994**, *116*, 4623.
(66) Woo, T. K.; Fan, L.; Ziegler, T. *Organometallics* **1994**, *13*, 2252.
(67) Erker, G.; Korek, U. Z. *Z. Naturforsch.* **1989**, *44B*, 1593.
(68) Brinkmann, P. H. P.; Prosenc, M. H.; Luinstra, G. A. *Organometallics* **1995**, *14*, 5481.
(69) Fandos, R.; Meetsma, A.; Teuben, J. H. *Organometallics* **1991**, *10*, 2665.
(70) Fandos, R.; Teuben, J. H.; Helgesson, G.; Jagner, S. *Organometallics* **1991**, *10*, 1637.
(71) Horton, A. D. *Organometallics* **1992**, *11*, 3271.
(72) Pattisiana, J. W.; Hissink, C. E.; de Boer, J. L.; Meetsma, A.; Teuben, J. H. *J. Am. Chem. Soc.* **1985**, *107*, 7758.

and **7**. Cycloadducts were not observed as intermediates in these reactions. Isolated azametallacyclobutene **3** rearranges thermally to the novel fulvene complex **5**.

Experimental Section

General Methods. Unless otherwise noted, all reactions and manipulations were carried out in dry glassware under a nitrogen or argon atmosphere at 20 °C in a Vacuum Atmospheres 553-2 drybox equipped with a MO-40-2 inert gas purifier, or using standard Schlenk techniques. The amount of O_2 in the drybox atmosphere was monitored with a Teledyne model #316 trace oxygen analyzer. For a description of other instrumentation and general procedures used, see ref 22.

Unless otherwise specified, all reagents were purchased from commercial suppliers and used without further purification. Phenyl- and trimethylsilylacetylene were distilled from $MgSO_4$ and stored over 4 Å molecular sieves. Acetylene gas was purified by passage through two −78 °C traps separated by a concentrated H_2SO_4 trap. Pentane and hexanes (UV grade, alkene free) were distilled from sodium benzophenone ketyl/tetraglyme under nitrogen. Benzene, toluene, diethyl ether, and THF were distilled from sodium benzophenone ketyl under nitrogen. Cyclohexane was distilled from calcium hydride under nitrogen. Deuterated solvents for NMR experiments were dried in the same way as their protiated analogues but were vacuum transferred from the drying agent. Tolyl azide[73] and $Cp^*_2Ti{=}NPh$[32] were prepared by literature methods. $Cp^*_2Ti(C_2H_4)$ was prepared by the literature method,[39] except that Cp^*_2TiCl[74] was used instead of $Cp^*_2TiCl_2$.

NMR Spectroscopy. NMR experiments were performed on a Brucker AMX spectrometer resonating at 300.13 MHz for ^{1}H, 75.42 MHz for ^{13}C, and 30.42 MHz for ^{15}N that was equipped with an inverse probe. The temperature in the probe was monitored using a thermocouple and was calibrated with an ethylene glycol standard.[75] Except where noted, all one- and two-dimensional experiments were acquired between 295 and 300 K. EXSY spectra were acquired at 273 K in phase-sensitive mode using the Brucker pulse program noesytp. A shifted sine bell window function was applied to the raw data set in both dimensions.[76] Integrations were performed on 1D slices through the cross-peaks of interest. The rate constants were determined from plots of cross-peak intensity vs mixing time as described elsewhere.[47]

Generation and Spectroscopic Characterization of 2. A solution of **1** (5.2 mg, 0.0127 mmol) in 0.5 mL toluene-d_8 was transferred to a J-Young NMR tube. Ferrocene (2.8 mg, 0.0150 mmol) was added as an internal standard. The sample was degassed at −195 °C under vacuum and backfilled to 1 atm with ethylene. The sample was transferred to a precooled NMR probe (−50.8 °C). Inspection of the ^{1}H NMR spectrum revealed that only ethylene and **2** were present in solution. ^{1}H NMR (toluene-d_8, −50 °C): δ 7.35 (m, 1H), 7.24 (m, 1H), 6.79 (m, 1H), 6.50 (m, 1H), 6.19 (m, 1H), 2.35 (m, 2H), 1.82 (m, 2H), 1.67 (s, 30H) ppm. ^{13}C{^{1}H} NMR (toluene-d_8, −50 °C): δ 129.7 (CH), 129.0 (CH), 123.1 (C), 120.7 (C), 120.2 (CH), 114.3 (CH), 109.4 (CH), 64.4 (CH_2), 25.5 (CH_2), 12.0 (CH_3) ppm.

Measurement of K_{eq} for the Equilibration of 1 and Ethylene with 2. A 1 mL volumetric flask was charged with **1** (11.1 mg, 0.0271 mmol) and Cp_2Fe (1.3 mg, 0.00699 mmol). The solution was brought to volume with toluene-d_8. A J-Young NMR tube was charged with 0.5 mL of this solution. The sample was frozen in liquid nitrogen and evacuated. Ethylene (0.0404 mmol) was condensed onto the frozen solution from a 23.58 mL bulb. ^{1}H NMR spectra were recorded at 10° increments from 253.3 to 283.2 K. A series of three one-pulse experiments separated by 5 min increments were acquired at each temperature, and the concentrations of **1**, **2**, and ethylene were determined by integration against the Cp_2Fe standard. The concentrations used to determine K_{eq} at each temperature were calculated by averaging the values for the three one-pulse experiments.

Table 4. Crystal Parameters for Complexes **3** and **6**

	$Cp^*_2Ti(NPhCH{=}CH)$ (**3**)	$Cp^*_2Ti(NHPh)C{\equiv}CPh$ (**6**)
empirical formula	$TiNC_{18}H_{37}$	$TiNC_{34}H_{41}$
fw (amu)	315.4	511.6
size (mm)	0.30 × 0.30 × 0.35	0.16 × 0.28 × 0.40
space group	$P2_12_12_1$ (No. 19)	$P2_1/c$
a (Å)	18.2307(4)	10.0432(16)
b (Å)	10.8656(2)	16.167(4)
c (Å)	12.1204(3)	17.541(4)
α (deg)	90.0	90.0
β (deg)	90.0	97.294(16)
γ (deg)	90.0	90.0
V (Å^3)	2400.9(2)	2825.0(18)
Z	4	4
d_{calcd} (g cm^{-3})	0.872	1.20
μ_{calcd} (cm^{-1})	3.52	3.2

$Cp^*_2Ti(N(Ph)CH{=}CH)$ (3). A Schlenk flask equipped with a magnetic stir bar was charged with **1** (122 mg, 0.297 mmol) in 40 mL of benzene. Acetylene gas was passed through the solution for 5 m. The solution was allowed to stir for an additional 15 m, and then the volatile materials were removed under reduced pressure. The red powder was extracted with hexanes (20 mL) and filtered. The volume of the filtrate was reduced to 8 mL in vacuo. Slow cooling to −50 °C overnight yielded 79.8 mg of blocky red crystals of **3** (61.7%) suitable for X-ray diffraction studies. IR (Nujol): 2771(w), 1587(s), 1459(s) 1326(s), 1236(m), 1168(m), 1114(m), 1020(m), 991(m), 776(s), 694(m) cm^{-1}. ^{1}H NMR (toluene-d_8, −40 °C): δ 7.27 (1H, m), 7.20 (1H, m), 7.08 (1 H, d, ^3J = 9 Hz), 7.02 (1 H, d, ^3J = 9 Hz), 6.93 (1 H, m), 6.72 (1 H, m), 5.93 (1 H, m), 1.67 (30 H, s) ppm. ^{13}C{^{1}H} NMR (toluene-d_8, −40 °C): δ 186.2 (CH), 129.6 (CH), 128.3 (CH), 126 (C), 120.8 (CH), 152 (C), 114.9 (CH), 111.8 (CH), 96.8 (CH), 12.2 (CH_3) ppm. MS (EI): m/z 435 (M^+). Anal. Calcd for $C_{28}H_{37}NTi$: C, 77.21; H, 8.58; N, 3.21. Found: C, 77.06; H, 8.58; N, 3.06.

$Cp^*_2Ti(NPhCD{=}CD)$ (3-d_2). Crystals of **1** (110.5 mg, 0.270 mmol) were dissolved in 8 mL of benzene and transferred to a glass bomb. The solution was degassed under vacuum, and C_2D_2 (0.681 mmol, 2.5 equiv) was condensed onto the frozen solution from a 138 mL bulb. The solution was stirred for 1 h at room temperature, and the volatile materials were removed under reduced pressure. The red powder was extracted into hexanes and filtered. The volume of the filtrate was reduced to 2 mL and cooled to −50 °C overnight to afford red crystals of **3-d_2** (60.3 mg, 51.1%). Examination by ^{1}H NMR spectroscopy showed that the doublets at 7.02 and 7.08 ppm, which correspond to the ring methine protons of **3**, were >99% deuterated.

X-ray structure of 3. A fragment of a red prismatic crystal of **3** having approximate dimensions of 0.30 × 0.30 × 0.35 mm was mounted on a glass fiber using Paratone N hydrocarbon oil. All measurements were made on a Siemens SMART diffractometer with a CCD area detector using graphite-monchromated Mo Kα radiation. All calculations were performed using the TEXSAN crystallographic software package of Molecular Structure Corporation.

Cell constants and an orientation matrix for data integration, obtained from a least-squares refinement using the measured positions of 8192 reflections in the range $3.00 < 2\theta < 45.00°$, corresponded to a primitive orthorhombic cell. The final cell parameters and specific data collection parameters for this data set are given in Tables 4 and 5. Inspection of the systematic absences of $h00$: $h \neq 2n$, $0k0$: $k \neq 2n$, and $00l$: $l \neq 2n$ uniquely determine the space group to be $P2_12_12_1$ (No. 19).

Data were integrated to a maximum 2θ value of 46.5° using the program SAINT with box parameters of 1.6 × 1.6 × 0.6°. The data were corrected for Lorentz and polarization effects. No decay correction was applied. The linear absorption coefficient, μ, for Mo Kα radiation is 3.5 cm^{-1}. The program XPREP was used to make an empirical absorption correction based on comparison of equivalent reflections and an ellipsoidal model of the absorption surface (T_{max} = 0.94, T_{min} = 0.88). The 10520 integrated reflections were averaged in space group $Pmmm$ to give 1995 unique reflections (R_{int} = 3.7%). These were used for solution of the structure. The structure was solved by direct methods and expanded using Fourier techniques. The correct enantiomer was

(73) Ugi, I.; Perlinger, H.; Behringer, L. *Chem. Ber.* **1958**, *91*, 2330.
(74) Pattiasina, J. W.; Heeres, H. J.; van Bolhuis, F.; Meetsma, A.; Teuben, J. H.; Spek, A. L. *Organometallics* **1987**, *6*, 1004.
(75) Amman, C.; Meier, P.; Merbach, A. E. *J. Magn. Reson.* **1982**, *46*, 319.
(76) In each case, the integration was checked before and after application of the window function. In no case were the integrals noticeably affected.

Table 5. Data Collection Parameters for $Cp^*_2Ti(NPhCH{=}CH)$ (**3**)

diffractometer	Siemens Smart
T (°C)	−98.0
radiation	Mo Kα (λ = 0.710 69 Å) graphite monochromated
take-off angle (deg)	6.0
crystal-to-detector distance (mm)	60
scan type	ω (0.3° per frame)
scan rate (s per frame)	30.0
$2\theta_{max}$ (deg)	46.4
no. of reflns collected	10569
no. of unique reflns	1995
no. of obsns ($I > 3.00\sigma(I)$)	10085
no. of variables	271
refln/param ratio	37.21
R	0.041
R_w	0.061
GOF	2.66
p-factor	0.031

Table 6. Data Collection Parameters for $Cp^*_2Ti(N(Ph)H)C{\equiv}CPh$ (**6**)

diffractometer	Enraf-Nonius CAD-4
T (°C)	−145
reflns measd	$+h, +k, +/-l$
scan width	$\Delta\theta = 0.80 + 0.35 \tan\theta$
scan speed (θ deg/min)	5.49
vert aperature (mm)	6.0
horiz aperature (mm)	$2.2 + 1 \tan\theta$
no. of reflns collected	3851
no. of unique reflns	3689
no. of reflns $F^2 > 3\sigma(F^2)$	2211
I_{min}/I_{max}	0.93
no. of variables	328
$R(F)$ (%)	4.64
$R_w(F)$ (%)	4.62
R_{all} (%)	9.81
GOF	1.423
p-factor	0.03

determined by refining both enantiomers against the unaveraged data. Hydrogen atoms were included in calculated positions and were not refined. The final cycle of full-matrix least-squares refinement was based on 10085 observed and unaveraged reflections ($I > 3.00\sigma(I)$) and 271 variable parameters and converged (largest parameter shift was 0.01 times its esd) with unweighted and weighted agreement factors of $R = 4.1\%$ and $R_w = 6.1\%$, respectively. The standard deviation of an observation of unit weight was 2.66. The weighting scheme was based on counting statistics and included a factor ($p = 0.031$) to downweight the intense reflections. The maximum and minimum peaks on the final difference Fourier map corresponded to 0.19 and −0.24 $e^-/Å^3$, respectively. A complete listing of intramolecular bond lengths and angles, positional parameters for all atoms, and anisotropic thermal parameters are available as Supporting Information.

$Cp^*(\eta^5,\eta^1\text{-}C_5Me_4CH_2CH{=}CH)TiN(Ph)(H)$ (5). Crystals of **3** (33 mg, 0.0758 mmol) were dissolved in 5 mL of benzene and transferred to a glass bomb. The solution was heated to 45 °C for 14 d, during which time the solution gradually turned brown. The volatile materials were removed under dynamic vacuum. The brown oil was redissolved in hexanes and filtered, and the volume of the filtrate was reduced to 0.5 mL. Cooling to −50 °C for 2 d gave **5** as a brown microcrystalline solid (18.8 mg, 57.0%). IR (cyclohexane): 3371(w), 1596(s), 1494(s), 1365, 1276(s), 1168, 1031, 1066, 997, 759, 759, 690 cm^{-1}. ^1H NMR (C_6D_6): δ 7.45 (1 H, m), 7.17 (1 H, m), 7.12 (1 H, m), 7.05 (1 H, m), 6.74 (1 H, m), 6.48 (1 H, s), 6.44 (1 H, m), 3.05 (1 H, m), 2.9 (1 H, m), 2.03 (3 H, s), 1.84 (3 H, s), 1.74 (15 H, s), 1.68 (3 H, s), 1.64 (3 H, s) ppm. $^{13}C\{^1H\}$ NMR (C_6D_6): δ 195.9 (CH), 157.2 (C), 150.6 (CH), 140.7 (C), 128.3 (CH), 121.0 (C), 120.4 (C), 119.9 (C), 119.7 (CH), 117.2 (CH), 115.7 (C), 113.5 (C), 33.2 (CH_2), 12.6 (CH_3), 12.4 (CH_3), 12.3 (CH_3), 11.9 (CH_3), 11.1 (CH_3), 10.3 (CH_3) ppm. HRMS (EI) m/z: calcd for $C_{28}H_{37}NTi$ 435.240547, found 435.240166.

$Cp^*_2Ti(NHPh)C{\equiv}CPh$ (6). Phenylacetylene (32 μL, 0.291 mmol) was added to a stirred solution of **1** (91.7 mg, 0.224 mmol) in toluene (20 mL). The solution turned black upon addition of the alkyne. The solution was stirred for 30 m, after which time the volatile materials were removed in vacuo. The brown powder was extracted with hexanes (15 mL) and filtered. Slow cooling to −50 °C gave **6** as dark red crystals (91.3 mg, 80.0%) suitable for X-ray diffraction studies. IR (Nujol): 3367(w), 1585(s), 1267(s), 1201(m), 1022(m), 856(m), 754(s), 692(s) cm^{-1}. ^1H NMR (C_6D_6): δ 7.65 (2 H, m), 7.39 (1 H, s), 7.17 (3 H, m), 7.01(3 H, m), 6.79 (1 H, m), 1.84 (30 H, s) ppm. $^{13}C\{^1H\}$ NMR (C_6D_6) δ 157.0 (C), 130.5 (CH), 128.3 (CH), 127.5 (CH), 126.0 (CH), 121.2 (C), 120.5 (CH), 119.0 (C), 118.0 (CH), 12.5 (CH_3) ppm. MS (EI): m/z 511 (M^+). Anal. Calcd for $C_{34}H_{41}NTi$: C, 79.81; H, 8.09; N, 2.74. Found: C, 79.79; H, 8.28; N, 2.68.

X-ray Structure of 6. Large red plate-like crystals of **6** were obtained by slow crystallization from hexanes at −50 °C. Fragments cleaved from some of these crystals were mounted on glass fibers using Paratone N hydrocarbon oil. The crystal was then transferred to an Enraf-Nonius CAD-4 diffractometer and centered in the beam. It was cooled to −145 °C by a nitrogen flow low-temperature apparatus which had been previously calibrated by a thermocouple placed at the same position. Crystal quality was evaluated via measurement of intensities and inspection of peak scans until a suitable sample was found. Final crystal size was 0.16 × 0.28 × 0.40 mm. Automatic peak search and indexing procedures yielded a monoclinic reduced primitive cell. Inspection of the Niggli values revealed no conventional cell of higher symmetry. The final cell parameters and specific data collection parameters for this data set are given in Tables 4 and 6.

The 3851 raw intensity data were converted to structure factor amplitudes and their esd's by correction for scan speed, background, and Lorentz and polarization effects. No correction for crystal decomposition was necessary. Inspection of the azimuthal scan data showed a variation $I_{min}/I_{max} = 0.93$ for the average curve. An empirical correction based on the observed variation was applied to the data. Inspection of the systematic absences indicated uniquely space group $P2_1/c$. Removal of systematically absent data left 3689 unique data in the final data set. The structure was solved by Patterson methods and refined via standard least-squares and Fourier techniques. In a difference Fourier map calculated following the refinement of all non-hydrogen atoms with anisotropic thermal parameters, peaks were found corresponding to the positions of all of the hydrogen atoms. Hydrogen atoms were assigned idealized locations and values of B_{iso} approximately 1.25 times the B_{eqv} of the atoms to which they were attached. Those attached to carbon atoms were included in structure factor calculations, but not refined. The amide hydrogen position was refined, but its thermal parameter was fixed as was done for the other hydrogen atoms. The final residuals for 328 variables refined against the 2211 data for which $F^2 > 3\sigma(F^2)$ were $R = 4.64\%$, wR = 4.62%, and GOF = 1.423. The R value for all 3689 data was 9.81%. The quantity minimized by the least-squares program was $\sum w(|F_o| - |F_c|)^2$, where w is the weight of a given observation. The p-factor, used to reduce the weight of intense reflections, was set to 0.03 throughout the refinement. The analytical forms of the scattering factor tables for the neutral atoms were used, and all scattering factors were corrected for both the real and imaginary components of anomalous dispersion.

Inspection of the residuals ordered in ranges of sin θ/λ, $|F_o|$, and parity and value of the individual indexes showed no unusual features or trends. The largest peak in the final difference Fourier map had an electron density of 0.30 $e^-/Å^3$ and the lowest excursion −0.14 $e^-/Å^3$. There was no indication of secondary extinction in the high-intensity low-angle data. Positional parameters for all atoms, anisotropic thermal parameters, as well as a complete listing of intramolecular bond lengths and angles are available as Supporting Information.

$Cp^*_2Ti(N(Ph)H)(C{\equiv}CSiMe_3)$ (7). Trimethylsilylacetylene (50.0 uL, 0.353 mmol) was added to a stirred benzene solution (20 mL) of **1** (43.0 mg, 0.105 mmol). The solution turned brown upon addition of the alkyne. The solution was stirred for 1 h, after which time the volatile materials were removed under dynamic vacuum. The resulting brown powder was extracted with hexanes (4 mL), filtered, and cooled to −50 °C to yield black needles of **7** (37.4 mg, 70.7%). IR (Nujol): 3369(w), 2721(w), 2019(s), 1585(s), 1261(s), 1241(s), 1172(w), 1070(w),

1022(m), 854(s), 754(s), 694(s) cm^{-1}. ^1H NMR (C_6D_6): δ 7.37 (1 H, s), 7.22 (2 H, m), 6.96 (2 H, m), 6.84 (1 H, m), 1.81 (s, 30H), 0.24 (9 H, s) ppm. $^{13}C\{^1H\}$ NMR (C_6D_6): δ 181.0 (C), 158.8 (C), 128.2 (CH), 127.9 (CH), 121.2 (C), 120.8 (CH), 119.0 (CH), 12.8 (CH_3), 1.3 (CH_3) ppm. MS (EI): *m*/*z* 507 (M^+). Anal. Calcd for $C_{31}H_{45}NSiTi$: C, 73.32; H, 8.95; N, 2.76. Found: C, 73.12; H, 9.05; N, 2.63.

Cp*$_2$Ti═NTol (17). A Schlenk flask was charged with Cp*$_2$Ti(C_2H_4) (226 mg, 0.653 mmol) and 20 mL of diethyl ether. A solution of *p*-tolyl azide (85 mg, 0.64 mmol) in 5 mL of diethyl ether was added using a syringe. Vigorous gas evolution ensued, and the solution turned from green to red within 1 min. The solution was stirred for 30 m, after which time the volatile materials were removed under dynamic vacuum. The resulting red powder was extracted with diethyl ether and cooled to −50 °C for 12 h to afford **17** as large red blocks (112 mg, 40.6%). ^1H NMR (C_6D_6): δ 1.87 (s, 30H), 2.30 (s, 3H), 6.16 (d, ^3J = 8.1 Hz, 2H), 7.01 (d, ^3J = 8.1 Hz, 2H) ppm. Anal. Calcd for $C_{27}H_{37}NTi$: C, 76.56; H, 8.82; N, 3.30. Found: C, 76.94; H, 9.06; N, 3.19.

Cp*$_2$Ti(N(tol)CH═CH) (18). A Schlenk flask equipped with a magnetic stir bar was charged with **17** (40.4 mg, 0.0953 mmol) in 30 mL of benzene. Acetylene gas was passed through the solution for 5 m. The solution was stirred for an additional 15 m, and the volatile materials were removed under vacuum. The red powder was extracted with hexanes (20 mL) and filtered, and the volume of the filtrate was reduced to 10 mL in vacuo. Slow cooling to −50 °C yielded blocky red crystals of **18** (17.3 mg, 63.6%). ^1H NMR (C_6D_6): δ 1.70 (s, 30H), 2.28 (s, 3H), 5.96 (broad, 1H), 7.0 (broad, 3H), 7.09 (d, 1H), 7.12 (d, 1H) ppm. $^{13}C\{^1H\}$ NMR (C_6D_6): δ 12.3 (CH_3), 20.8 (CH_3), 97.9 (CH), 120.8 (C), 123.7 (C), 148.9 (C), 187.5 (CH) ppm. Due to slow rotation of the tolyl group, the tolyl methine resonances were not resolved in the ^{13}C spectrum. Anal. Calcd for. $C_{29}H_{39}NTi$: C, 77.47; H, 8.76; N, 3.11. Found: C, 77.19; H, 8.73; N, 3.11.

Acknowledgment. We thank the National Institutes of Health (grant no. R37-GM25459) for generous financial support of this work. We are grateful to Dr. Graham Ball for helpful discussions. We also thank Dr. F. J. Hollander, director of the University of California Berkeley College of Chemistry X-ray diffraction facility (CHEXRAY), for solving the crystal structures of **3**, **5**, and **6**.

Supporting Information Available: Tables of positional and thermal parameters and intramolecular bond lengths and angles for the structures of **3** and **6**, details of the crystal structure determination of **5** including ORTEP drawings showing full atomic numbering, crystal and data collection parameters, positional parameters and their estimated standard deviations, and intramolecular distances and angles (18 pages, print/PDF). See any current masthead page for ordering information and Web access instructions.

JA981489N